METROLOGICAL CHARACTERIZATION OF A LASER-CAMERA 3D VISION SYSTEM THROUGH PERSPECTIVE-N-POINT POSE COMPUTATION AND MONTE CARLO SIMULATIONS

Paolo Brambilla*[1], Chiara Conese[1], Davide M. Fabris[1], Marco Tarabini[1]

[1] Politecnico di Milano, Mechanical Engineering Dept., Via La Masa 1, 20156 Milan, Italy

Technical Commission II

KEY WORDS: 3D vision, laser profilometer, points projection, camera calibration, sensor fusion, Monte Carlo Method, Design of Experiments.

ABSTRACT:

This study focuses on the metrological characterization of a 3D vision system consisting in the fusion of a CMOS camera sensor with a 2D laser scanner for contactless dimensional measurements. The purpose is to obtain an enhanced measurement information as a result of the combination of two different data sources. On one side, we can estimate the pose of the target measurand by solving the well-known Perspective-n-Point (PnP) problem from the calibrated camera. On the other side, the 2D laser scanner generates a discrete point cloud which describes the profile of the intercepted surface of the same target object. This solution allows to estimate the target's geometrical parameters through the application of fit-to-purpose algorithms that see the data acquired by the overall system as their input. The measurement uncertainty is evaluated by applying the Monte Carlo Method (MCM) to estimate the uncertainty deriving from the Probability Distribution Functions (PDF) of the input variables. Through a Design of Experiments (DOE) model the effects of different influence factors were evaluated.

1. INTRODUCTION

There are different optical methods that can be used for non-contact dimensional measurements, but only a few of them can be used in presence of high-temperature measurands (Marcotuli 2022). The most widely used vision systems used by steel manufacturing industries are based on calibrated cameras, on stereoscopic vision and on 2D profilometers.

Profilometers typically use blue or green lasers and triangulation in order to reconstruct a part of the section of the workpiece. These sensors allow obtaining uncertainties in the order of mm when measuring diameters or linear dimensions of approximately 1 m. Standard cameras can be used to detect the diameter or the silhouette of the objects, with accuracies that are 1 order of magnitude larger than those of the profilometers; however, camera allows retrieving dense information about the specimen, allowing to reconstruct the entire geometry of the workpiece during its rotation(Chao et al. 2015; Ghiotti et al. 2015; Nye, Elbadan, and Bone 2001; Zhang et al. 2014).

The main idea behind this work is to use data fusion in order to combine the density of information of the camera-based measurements with the accuracy of 2D profilometers. This requires the knowledge of the relative 3D transformation among the profilometer and the camera, that can be determined with the application of the Perspective-n-Point (PnP) model (Fischler and Bolles 1981; Lu 2018). The problem is widely used in machine vision applications (Chunduru et al. 2021; Fabris et al. 2021; Ghosh and Mudur 1995; Luppino et al. 2022; Wu 2006) and consists in solving the rotational and translational vectors that minimize the reprojection error of points belonging to the 3D real world frame into the 2D image plane. In order to increase the reliability of the pose estimation, fiducial marker systems can be used (Fiala 2005; Rekimoto and Ayatsuka 2000) instead of the classic feature-based methods for the object tracking. These methods rely on the identification of ad-hoc designed marker, typically flat and square shaped, physically mounted on the object to be tracked.

The measurement uncertainty of the deriving system can be evaluated by applying the Monte Carlo Method (MCM) as it is prescribed by the ISO GUM Supplement 1 (Joint Committee for Guides in Metrology (JCGM) 2008) and Supplement 2 (Joint Committee for Guides in Metrology (JCGM) 2011). This method exploits the MCM for estimating the uncertainty deriving from the Probability Distribution Functions (PDF) of the input variables and has been applied in several works and studies (Cox and Siebert 2006; Fabris et al. 2022; Ghiani, Locci, and Muscas 2004; Moschioni et al. 2013; Nuccio and Spataro 2008).

Section 2 describes the method used for the projection of the laser point clouds to the image plane and for the estimation of its uncertainty starting from the most influencing input parameters. Related results are shown and discussed in Section 3.

2. METHOD

2.1 Projection of points from laser to image reference frame

Figure 1 shows the logical scheme used for the projection of a generic point belonging to the laser points cloud (P) to the image plane (Q). The roto-translational projection matrix M_P is defined by the formula reported in Equation 1.

$$M_P = M_I \cdot M_E \cdot M_L \quad (1)$$

Where:

- M_P is the overall projection matrix from the Laser Reference System LRS (x_L, y_L, z_L) to the Image Plane (u, v).
- M_L is the transportation matrix from the LRS to the World Reference System WRS (x_W, y_W, z_W). The WRS is considered as the structure supporting the

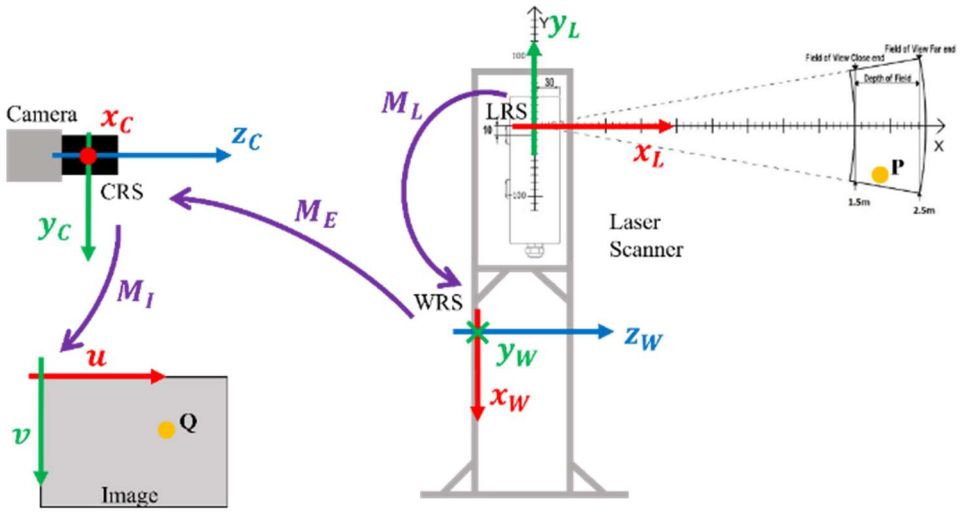

Figure 1. Schematic of the developed 3D vision system: LRS is the Laser Reference System, WRS is the World Reference System, CRS is the Camera Reference System, P is a generic 3D point expressed in LRS, Q is the projection of point P in the image plane.

laser, whose position is identified by a marker attached to the structure itself.

- M_E is the Extrinsic Matrix obtained solving the Perspective-n-Points problem identifying the relative pose of the marker on the laser structure with respect to Camera Reference System CRS (x_C, y_C, z_C). using the *"Infinitesimal Plane-Based Pose Estimation"* (IPPE) algorithm proposed by (Collins and Bartoli 2014) and implemented in OpenCV.
- M_I is the Intrinsic Matrix obtained from the camera calibration procedure performed using a chessboard (Zhang and Member 2000). It is completely defined by the focal distances f_x and f_y and the coordinates of the image principal point u_0 and v_0.

The complete Equation used to project the points from the LRS to the image plane is reported in Equation 2.

$$\begin{bmatrix} u \\ v \\ 1 \end{bmatrix} = \frac{1}{z_C} [M_I|0\,][M_E][M_L] \begin{bmatrix} x_L \\ y_L \\ 0 \\ 1 \end{bmatrix} \quad (2)$$

Where M_I is a three-rows and three-columns matrix.
M_E and M_L are both four-rows and four-columns matrices as shown in Equations 3.

$$M_I = \begin{bmatrix} f_x & s & u_0 \\ 0 & f_y & v_0 \\ 0 & 0 & 1 \end{bmatrix}$$

$$M_E = \begin{bmatrix} R_{xx_E} & R_{xy_E} & R_{xz_E} & t_{x_E} \\ R_{yx_E} & R_{yy_E} & R_{yz_E} & t_{y_E} \\ R_{zx_E} & R_{zy_E} & R_{zz_E} & t_{z_E} \\ 0 & 0 & 0 & 1 \end{bmatrix} \quad (3)$$

$$M_L = \begin{bmatrix} R_{xx_L} & R_{xy_L} & R_{xz_L} & t_{x_L} \\ R_{yx_L} & R_{yy_L} & R_{yz_L} & t_{y_L} \\ R_{zx_L} & R_{zy_L} & R_{zz_L} & t_{z_L} \\ 0 & 0 & 0 & 1 \end{bmatrix}$$

z_C is the coordinate of the point P on the z axis of the CRS, i.e. the distance of the point from the optical centre of the camera.

The mounting position of the marker on the back of the laser scanner support is known, thus the nominal roto-translation matrix $\widehat{M_L}$ can be computed.

2.2 Estimation of Uncertainty

At this stage, we concentrate on the study of M_L matrix, that is the one that, in principle, should be responsible of the larger contribution in the overall uncertainty. Its uncertainty depends on three factors:

i. Uncertainty about the real position of the origin optical point of the LRS
ii. Uncertainty about the real orientation of the LRS
iii. Lack of precision in the marker mounting on the structure supporting the laser

The roto-translation matrix M_L described in Equation 3 contains a three-rows and three-columns rotational matrix (R_L), a three rows translation vector (t_L) and a last row with a three-columns zeroes vector and a 1.
Elements of the matrix M_L, i.e. elements of the translation vector t_L and of the rotation matrix R_L are associated to their measurement uncertainties. Uncertainty on the positioning along the three axes directly affect the value in the translation vector, while the perturbation on the rotation matrix is computed starting from the uncertainty among the three axes in the rotation vector r_L (Equation 4).

$$r_L = \begin{bmatrix} r_{x_L} \\ r_{y_L} \\ r_{z_L} \end{bmatrix} \quad (4)$$

Equation 5 reports the passages to compute the rotation matrix (R_L), that is necessary to compute the matrix M_L, given the rotation vector r_L.

$$\begin{aligned} \theta &= norm(r_L) \\ r_L &= \frac{r_L}{\theta} \\ R_L &= cos(\theta)I + \big(1 - cos(\theta)\big) r_L {r_L}^T + sin(\theta) {}^* R \end{aligned} \quad (5)$$

$$R = \begin{bmatrix} 0 & -r_{z_L} & r_{y_L} \\ r_{z_L} & 0 & -r_{x_L} \\ -r_{y_L} & r_{x_L} & 0 \end{bmatrix}$$

2.3 Simulations

The setup used to perform the experiment is composed by a UI-3060CP Rev. 2 camera from IDS GmbH, with a 1216x1936 pixel monochromatic sensor equipped with a 12mm lens and a O2DS laser scanner from DSE. The distance from the laser and the acquired profile is 2m while the camera is positioned 3m behind the laser. The field of view of the camera at the distance of the acquired profile is 4.7m wide and 3m high.
The relative importance of the different factors on the overall measurement uncertainty can be obtained with the simultaneous use of factorial Design of Experiments and Monte Carlo simulations. With this approach, it is possible to estimate the contribution of each influencing factor (IF) on the overall uncertainty.
The quantities affected by uncertainty are the three elements of the translation vector t_L and the three elements of the rotation vector r_L, so a total of six IFs are considered. The vector containing the nominal value of the quantity is defined as in Equation 6.

$$\hat{X} = [\hat{t}_{x_L}, \hat{t}_{y_L}, \hat{t}_{z_L}, \hat{r}_{x_L}, \hat{r}_{y_L}, \hat{r}_{z_L}] \quad (6)$$

Each of the IF can assume two discrete levels of uncertainty (Low or High). Every configuration is perturbed adding to the nominal values a deviation sampled from six Gaussian distributions with zero mean and standard deviation given by the combination of uncertainty levels. A total of $2^6 = 64$ configurations of uncertainty were tested.
The selected numerical values are: 0.5 mm for the Low uncertainty and 5 mm for the High uncertainty of the three displacements, 0.1° for the Low uncertainty and 1° for the High uncertainty of the three orientations.
For each input uncertainty configuration, we applied the Monte Carlo method with a vector (Δ) of 10000 samples defining the probability density function with the specific uncertainties combinations. For each configuration, 10000 perturbed X^* vectors are computed as in Equation 7.

$$X^* = \hat{X} + \Delta$$
$$\Delta = [\delta_{tx_L}, \delta_{ty_L}, \delta_{tz_L}, \delta_{rx_L}, \delta_{ry_L}, \delta_{rz_L}] \quad (7)$$

Where δ_{i_L} is the value of noise related to the quantity i sampled from a Gaussian distribution, the six values of noise make up the noise vector (Δ).
Starting from X^*, the perturbed translation vector t_L^* and perturbed rotation matrix R_L^* are built and the perturbed roto-translation matrix M_L^* is used in Equation 2 to project the Laser points into the Image plane.

2.4 Evaluation Metrics

In each simulation 200 points are reprojected from LRS to Image and the RMSE is computed according to the following equation (Equation 8)

$$RMSE = \sqrt{\frac{1}{200}\sum_{i=1}^{200}(Q^* - \hat{Q})^2} \quad (8)$$

Where:

- Q^* is the position of the projected point using the perturbated roto-translation matrix
- $\hat{Q}$ are the coordinates of the projected point using the nominal roto-translation matrix

3. RESULTS

Figure 2 illustrates an example of a scene seen from the camera with the points acquired by the laser scanner projected in the image with green crosses. One the lower left part of the picture the laser case with the marker attached on the back is visible. The black area near the image border is due to the distortion removal procedure.
On the Upper left corner of the picture is reported an enlargement of the top points of the profile.

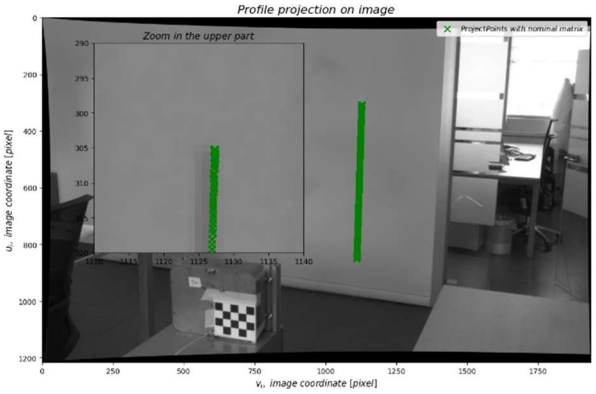

Figure 2. Image of the scene taken from the camera; the green points represent the points acquired by the laser reprojected on the image plane. On the upper left side an enlargement of the top points of the profile is reported

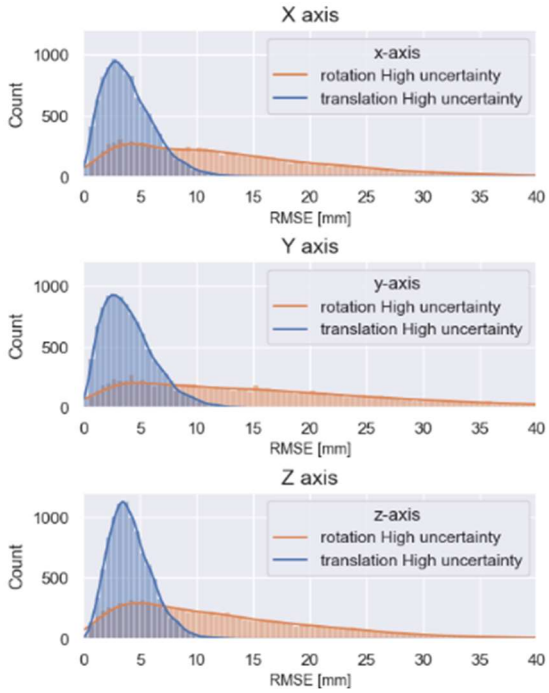

Figure 3. shows the comparison of the RMSE distribution on each axis when the translational component or the rotational component is affected by High uncertainty, while all the other are affected by a Low uncertainty

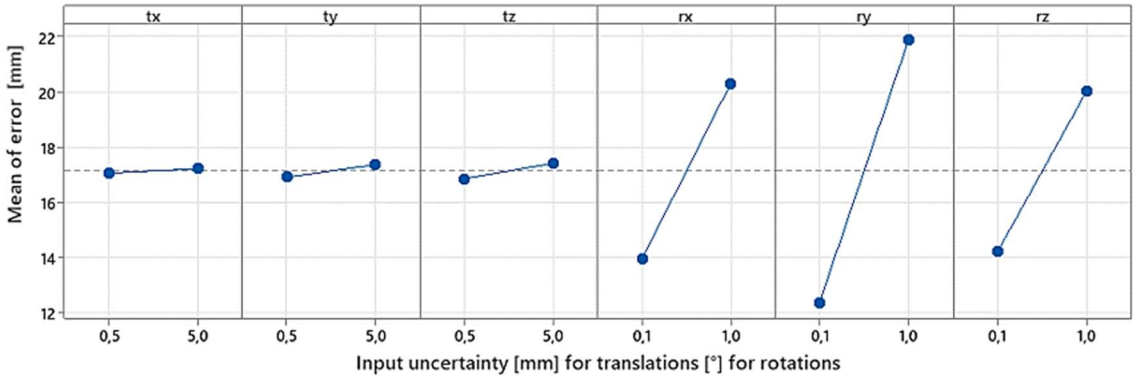

Figure 4. Main Effects Plot of the RMSE for the analysed levels of uncertainty.

The developed Factorial Regression Model is characterized by an adjusted correlation coefficient (R^2) equal to 98.4% and a standard deviation of 0.84mm. In figure 4 is reported the Main Effects Plot for the RMSE for each of the six IFs. The average RMSE value is 17.3mm.
Figure 5 shows an application example, where a profile different from a line is projected on the image.

4. DISCUSSION AND CONCLUSION

Results of Monte Carlo simulations allowed estimating the measurement uncertainty of the position of the 2D point cloud measured by the profilometer in the image plane of a camera observing the profilometer and the measurand.
The value of uncertainty is compatible with hardware components of the setup, their resolution and the camera field of view (FoV), considering that at the distance of the profile from the camera the pixel dimension is 2.4mm. The average RMSE value correspond to the 0.36% of the FoV width, moreover this order of magnitude on the positioning RMSE can be considered negligeable if compared to the total FoV.
Uncertainty is governed by the rotation components as can be seen in Figure 4 and further studies are required to determine the pose of the marker minimizing the error on the orientation. Further studies will also focus on the implementation of a calibration procedure aimed at the minimization of the RMSE to adjust the roto-translation matrix M_L between the laser and the world reference system to compensate possible error given by the manual computation of those parameters.

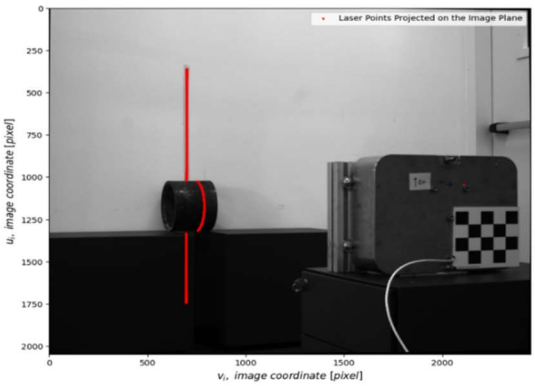

Figure 5. Application example where a profile different from a line is acquired

REFERENCES

Chao, Bi, Qu Xinghua, Liu Yong, Liu Yaping, and Liu Jingliang. 2015. "Dimensional Measurement of Small Hot Pieces Based on a Monochrome CCD." *Procedia Engineering* 99(2011):1158–63.

Chunduru, Vaishnav, Mrinalkanti Roy, N. S. Dasari Romit, and Rajeevlochana G. Chittawadigi. 2021. "Hand Tracking in 3D Space Using MediaPipe and PnP Method for Intuitive Control of Virtual Globe." *IEEE Region 10 Humanitarian Technology Conference, R10-HTC* 2021-Septe.

Collins, Toby and Adrien Bartoli. 2014. "Infinitesimal Plane-Based Pose Estimation." *International Journal of Computer Vision* 109(3):252–86.

Cox, Maurice G. and Bernd R. L. Siebert. 2006. "The Use of a Monte Carlo Method for Evaluating Uncertainty and Expanded Uncertainty." *Metrologia* 43(4).

Fabris, Davide Maria, Alice Meldoli, Remo Sala, Paolo Salina, and Marco Tarabini. 2021. "Metrological Characterization of Measurement Systems through Monte Carlo Simulations, Design of Experiments and Robotic Manipulation." in *IEEE International Workshop on Metrology for Industry 4.0 (MetroInd4.0&IoT)*.

Fabris, Davide Maria, Alice Meldoli, Paolo Salina, Remo Sala, and Marco Tarabini. 2022. "Optimized Design and Characterization of a Non-Linear 3D Misalignment Measurement System." *IEEE Transactions on Instrumentation and Measurement* 71.

Fiala, Mark. 2005. "ARTag, a Fiducial Marker System Using Digital Techniques." *Proceedings - 2005 IEEE Computer Society Conference on Computer Vision and Pattern Recognition, CVPR 2005* II:590–96.

Fischler, Martin A. and Robert C. Bolles. 1981. "RANSAC: Random Sample Paradigm for Model Consensus: A Apphcatlons to Image Fitting with Analysis and Automated Cartography." *Graphics and Image Processing* 24(6):381–95.

Ghiani, Emilio, Nicola Locci, and Carlo Muscas. 2004. "Auto-Evaluation of the Uncertainty in Virtual Instruments." *IEEE Transactions on Instrumentation and Measurement* 53(3):672–77.

Ghiotti, A., A. Schöch, A. Salvadori, S. Carmignato, and E. Savio. 2015. "Enhancing the Accuracy of High-Speed Laser Triangulation Measurement of Freeform Parts at Elevated Temperature." *CIRP Annals - Manufacturing Technology* 64(1):499–502.

Ghosh, P. K. and S. P. Mudur. 1995. "Three-Dimensional Computer Vision: A Geometric Viewpoint." *The Computer Journal* 38(1):85–86.

Joint Committee for Guides in Metrology (JCGM). 2008.

"Evaluation of Measurement Data – Supplement 1 to the Guide to the Expression of Uncertainty in Measurement – Propagation of Distributions Using a Monte Carlo Method." 73.

Joint Committee for Guides in Metrology (JCGM). 2011. "Evaluation of Measurement Data – Supplement 2 to the 'Guide to the Expression of Uncertainty in Measurement' – Extension to Any Number of Output Quantities." *Iso/Iec* 102.

Lu, Xiao Xin. 2018. "A Review of Solutions for Perspective-n-Point Problem in Camera Pose Estimation." *Journal of Physics: Conference Series* 1087(5).

Luppino, Giada, Lisa Bosisio, Chiara Conese, Davide Maria Fabris, and Marco Tarabini. 2022. "Metrology of a Monocular Vision System for Markers Localization and Tracking." *2022 IEEE International Workshop on Metrology for Industry 4.0 and IoT, MetroInd 4.0 and IoT 2022 - Proceedings* 6–10.

Marcotuli, Valerio. 2022. "A Contactless Measurement System for High Temperature Shaft Manufacturing in Open Die Forging." *Politecnico Di Milano, Doctoral Thesis*.

Moschioni, G., B. Saggin, M. Tarabini, J. Hald, and J. Morkholt. 2013. "Use of Design of Experiments and Monte Carlo Method for Instruments Optimal Design." *Measurement: Journal of the International Measurement Confederation* 46(2):976–84.

Nuccio, Salvatore and Ciro Spataro. 2008. "Uncertainty Management in the Measurements Performed by Means of Virtual Instruments." *AMUEM 2008 - IEEE Workshop on Advanced Methods for Uncertainty Estimation Measurement Proceedings* (August):40–45.

Nye, T. J., A. M. Elbadan, and G. M. Bone. 2001. "Real-Time Process Characterization of Open Die Forging for Adaptive Control." *Journal of Engineering Materials and Technology, Transactions of the ASME* 123(4):511–16.

Rekimoto, Jun and Yuji Ayatsuka. 2000. "CyberCode: Designing Augmented Reality Environments with Visual Tags." *Proceedings of DARE 2000 on Designing Augmented Reality Environments* 1–10.

Wu, Yihong. 2006. "PnP Problem Revisited." *Journal of Mathematical Imaging and Vision* 24(1):131–41.

Zhang, Yu Cun, Jun Xia Han, Xian Bin Fu, and Fu Li Zhang. 2014. "Measurement and Control Technology of the Size for Large Hot Forgings." *Measurement: Journal of the International Measurement Confederation* 49(1):52–59.

Zhang, Zhengyou and Senior Member. 2000. "A Flexible New Technique for Camera Calibration." *IEEE Transactions on Pattern Analysis and Machine Intelligence* 22(11):1330–34.